Technical Paper 666-A.
St. Anthony Falls Laboratory

STATISTICAL GEOMETRY AND DYNAMICS OF BRAIDED RIVERS

Chris Paola
St. Anthony Falls Laboratory, University of Minnesota,
Minneapolis MN 55414 USA
Department of Geology and Geophysics, University of Minnesota,
Minneapolis MN 55455 USA

Efi Foufoula-Georgiou
St. Anthony Falls Laboratory, University of Minnesota,
Minneapolis MN 55414 USA

ABSTRACT

The statistical geometry of braided rivers has been studied from a variety of viewpoints, from simple random walks through dynamical-systems theory to analysis of static and dynamic scaling of river planform. The most important results to date are that (1) methods based on statistical geometry are a useful way of testing models, and (2) braided rivers show both anisotropic spatial scaling and time-space dynamic scaling such that the evolution of large areas looks like the evolution of smaller areas run in slow motion. Specifically, the evolution of an area with length scale L_2 is statistically indistinguishable from that of a smaller area with length scale L_1 provided the time step is increased (i.e. the evolution is slowed down) as approximately $(L_2/L_1)^{1/2}$. This implies that the likelihood of large-scale changes over long time scales can be estimated from measurements of the distribution of small-scale changes over short time intervals.

1. INTRODUCTION

A braided river comprises a network of interconnected channels that evolves temporally in a way that seems to be predictable only over relatively short intervals. The complexity and unpredictability of braided rivers invite statistical analysis of their dynamics. Our goal here is to review some of the statistical-geometric measures that have been applied to braided rivers, with emphasis on scaling relations (relations that apply to a range of scales under appropriate normalisation), and to outline how these can be related to the underlying physics of the river network. We will also discuss the utility of these measures in evaluating models of braiding.

Early attempts to characterise the geometry of braided rivers focused on basic topological measures such as mean link length and number of channels (the so-called 'braid index'). In an important early contribution, Howard *et al.* (1970) showed how a very simple random walk model could reproduce many of these averaged network quantities. The model contained no physics, and could not evolve with time, suggesting that none of the simple topological measures were very discriminating means of testing models.

Two more involved approaches have been developed to analyse the geometry of braided rivers since then. One is based on "dynamical systems theory"; the basic idea is to look for spatial structure in integral quantities such as total channel width, treating spatial sequences as time series (Murray and Moeckel, 1997; Murray and Paola, 1996). The second approach is based on the ideas of static and dynamic scaling. The basis for this approach is the apparent self-similarity of braided rivers, both for small and large systems and for different spatial and temporal scales within a given system (Nykanen *et al.*, 1998; Sapozhnikov and Foufoula-Georgiou, 1995; Sapozhnikov and Foufoula-Georgiou, 1996; Sapozhnikov and Foufoula-Georgiou, 1997; Sapozhnikov and Foufoula-Georgiou, 1999).

2. MEASURES OF STATISTICAL GEOMETRY

2.1 Dynamical-systems based approach

In view of the apparent insensitivity of traditional simple network statistics when used for model testing, Murray *et al.* (1996) proposed an approach based on dynamical systems theory. Most of these approaches have been developed for time series of a single scalar variable, and in general they are associated with the concept informally known as chaos: apparently unpredictable behaviour in deterministic systems. The original idea of most of the dynamical-systems methods of time-series analysis (Weigend and Gershenfeld, 1994) was to search for evidence of low-dimensional chaos and, if it was found, to characterise it quantitatively. It turns out that true low-dimensional chaos is quite rare in nature. Nonetheless, dynamical-systems statistical approaches may be useful in comparing systems with one another or with models, as long as one is careful not to interpret the results as necessarily defining true 'attractors'. Since braided rivers are clearly chaotic, in the broad sense of being deterministic systems that show apparently unpredictable behaviour, in principle the same techniques could be applied to time series from braided rivers. Unfortunately, dynamical-systems methods tend to be data-intensive: 500 points are often considered a minimum for analysis. Most natural braided rivers evolve slowly enough that obtaining such a long time series while maintaining stationary conditions is not practical. The idea can readily be adapted to spatial series, however, by assuming that causality in braided rivers *in general* proceeds from upstream to downstream (though this assumption is a reasonable starting point, it may not be true—see Seminara *et al* (2001) for further discussion of upstream and downstream influences in river systems). The limitations of available data suggest using a relatively simple planform measure of geometry. Murray and Paola (1996) proposed total (summed) channel width as a physically meaningful variable for which long spatial series can readily be obtained from air photos.

The spatial series so obtained is then treated as a time series. For a spatial series of widths $b_1, b_2, \ldots b_n$, a series of m-dimensional vectors $V_{1 \ldots n-m+1}$ is formed as $V_1 = \{ b_1, b_2, \ldots b_m \}$. These vectors then form a path in m-dimensional space (a 'state space': Figure 1). The structure of this path reflects the way in which downstream widths are influenced by upstream widths; clusters, for instance, represent preferred width sequences. For chaotic systems, such vector paths define the attractor of the dynamics, provided the vector dimension (i.e. the length of the width sequences) is at least equal to the true dimension of the attractor. Unfortunately, at this point all indications are that braided rivers are high-dimensional. For instance, point trajectories in low-dimensional plots such as Figure 1 are not unique; rather the paths intersect one another (Murray and Paola, 1996). In this case, low-dimensional plots cannot define the attractor. However, it is still possible that useful information can be extracted from them. In particular, state-space plots might still be an avenue for comparing field, laboratory, and theoretical braid patterns quantitatively. To do this, Murray and Moeckel (1997) proposed a method based on thinking of the state-space plot simply as a probability density in m-dimensional space. Their method is illustrated in Figure 1. A state-space plot is constructed as explained above for each system to be compared. Each state-space plot is then converted to a discrete probability distribution by dividing it into m-dimensional volumes and assigning each volume a probability equal to the number of points it contains normalised by the total number of points. Then the distributions are compared, pairwise, via the "transportation distance": a measure of the minimum amount one distribution has to be reconfigured to convert it to the other one. This is illustrated in Figure 1. This method turns out to be relatively insensitive to outliers, and to the volume size chosen for discretisation, compared with other available methods.

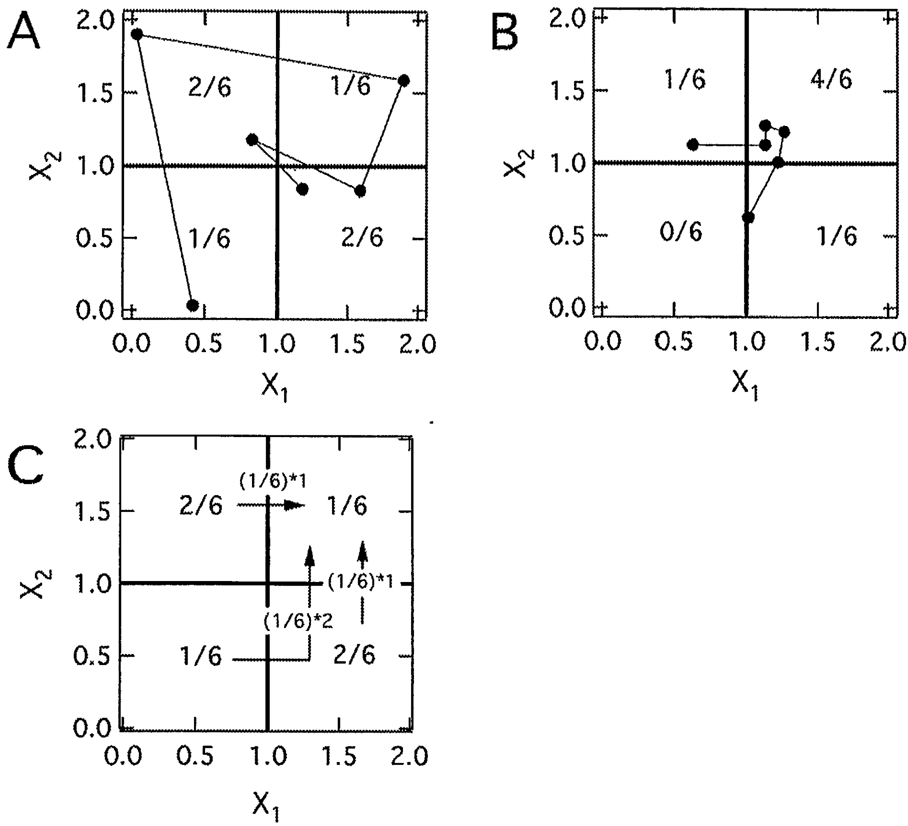

Figure 1. **(a,b) Example state-space plots from (a) a succession of random numbers and (b) a succession of widths (normalised by mean width) measured from an aerial photograph of the Sunwapta River, Alberta, Canada. In each case x_2 is the value of the variable following x_1. The two-dimensional probability density has been crudely discretised into four boxes. (c) Computation of the 'transport distance' proposed by Murray and Moeckel (1997) for comparing state-space plots quantitatively. The transport distance is the minimum weighted distance that probabilities in (a) must be shifted to reproduce the distribution in (b), in this case 0.667 (4/6).**

2.2 Spatial scaling

Well-developed braided rivers often show internal geometric similarity in the sense that parts of the network seem to resemble the network as a whole. For example, Figure 2 illustrates that a small part of the river looks statistically similar to a larger part under appropriate rescaling of the spatial coordinates. Moreover, visual comparison of spatial patterns of different braided rivers often reveals that there are apparent statistical similarities between one braided river and another. For example, Figure 3 displays digitised images of three braided rivers: the Brahmaputra River in Bangladesh, and the Aichilik and Hulahula Rivers in Alaska. Despite the different natural scales of these systems and their different slopes and bed materials (Table 1), when projected to the same scale as in Figure 3 they all appear to have statistically similar geometry.

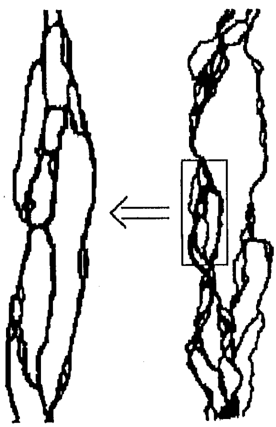

Figure 2. **Static scaling: a small part of a braided-river network resembles the overall pattern.**

Table 1. **Hydrological and geomorophological characteristics of three natural braided rivers.**

	Brahmaputra	Aichilik	Hulahula
Reach width, km	15	0.5	0.7
Reach length, km	200	6.4	20
Mean channel depth, m	5	1	1
Slope	7.7×10^{-5}	10^{-3}	7×10^{-4}
Braiding index*	3.8	6.8	5.2
Predominant bed material	sand	gravel	gravel

*average number of channels per lateral transect

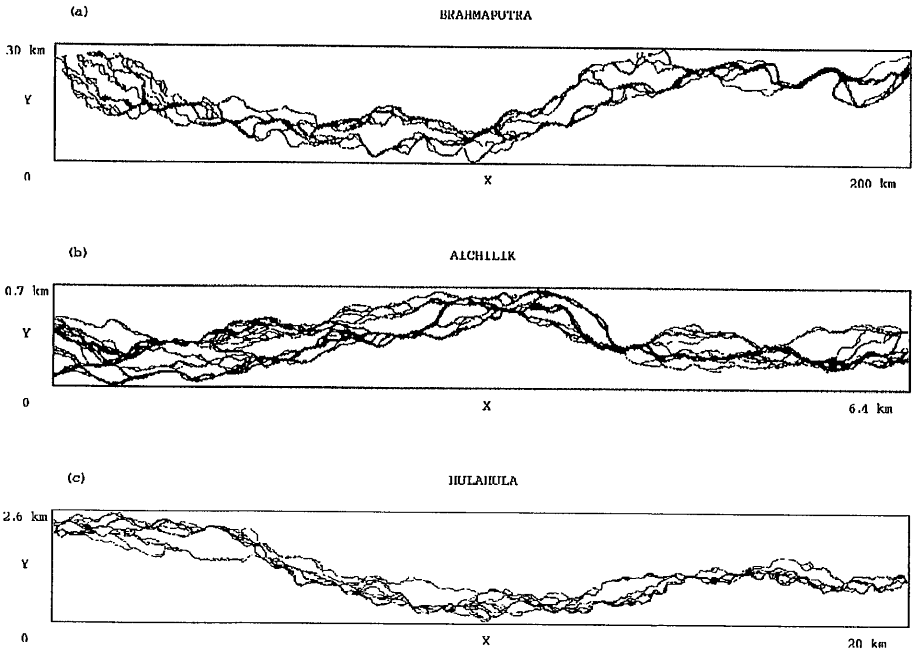

Figure 3. Images of the Brahmaputra River, Bangladesh, and the Aichilik and Hulahula Rivers, Alaska, projected to the same scale for comparison. Note that although the Brahmaputra is much larger than the two Alaskan ones, and is sand-bed rather than gravel-bed, all three are statistically similar when scaled appropriately.

Statistical similarity or scale invariance is an important aspect of the geometry of a system and, as will be discussed below, offers clues as to the underlying physics of the system. When the geometrical properties of an object exhibit the same scaling relations in all directions (referred to as isotropic scaling) the object is called a 'self-similar' fractal. However, when the properties scale differently in different directions (referred to as anisotropic scaling) the object is called a 'self-affine' fractal. Since braided rivers exhibit a preferred direction (the direction of downstream flow) it is natural to expect anisotropy. The first analysis of geometric statistical similarity or anisotropic spatial scaling in braided rivers was performed by Sapozhnikov and Foufoula-Georgiou (1996), based on a methodology they had developed previously (Sapozhnikov and Foufoula-Georgiou, 1995). This methodology is called the Logarithmic Correlation Integral (LCI) method and is presented briefly in the Appendix for completeness.

Anisotropic scale invariance is characterised by two fractal exponents, denoted by ν_x and ν_y, where x represents the direction of the average flow and y the cross-flow direction. Briefly, the LCI method computes the "mass" $M(X,Y)$ (defined as the number of pixels covered by water) within rectangles of size $X \times Y$ for various rectangle sizes. Then these computations are projected in the log-space, i.e., the function $z(x,y) \equiv \log M(\log x, \log y)$ is formed and its derivatives with respect to x and y are computed (this is called the Logarithmic Correlation Integral function). As shown in Sapozhnikov and Foufoula-Georgiou (1995), a linear plot of $\partial z(x,y)/\partial y$ vs. $\partial z(x,y)/\partial x$ indicates the presence of spatial scale invariance, and the anisotropic scaling exponents ν_x and ν_y can be estimated from the slope and intercept of this plot. Figure 4 shows plots of $\partial z/\partial y$ versus $\partial z/\partial x$ for the three braided rivers shown in Figure 3. The points on the plots show a good linear dependence indicating the presence of self-affinity in all three rivers. The values of the scaling exponents ν_x and ν_y were found to have similar values for all three rivers: $\nu_x = 0.74$ and $\nu_y = 0.51$ for the Brahmaputra; $\nu_x = 0.72$ and $\nu_y = 0.51$ for the Aichilik; and $\nu_x = 0.74$ and $\nu_y = 0.52$ for the Hulahula.

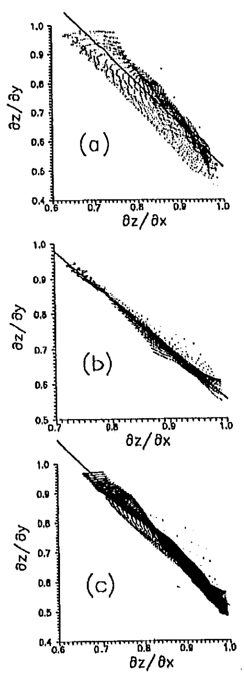

Figure 4. **Logarithmic Correlation Integral (LCI) plots for the three braided rivers shown in Figure 3.**

Sapozhnikov and Foufoula-Georgiou (1996) postulated that the presence of statistical spatial scaling in the morphology of braided rivers is an indication that the underlying mechanisms responsible for the formation of braided rivers are universal and the same at all scales. If these mechanisms (e.g. see Murray and Paola (1994)) were disturbed at any scale by external controls, such as for example mountain ranges or predominant flow paths, then spatial scaling would not be expected to hold. Indeed, analysis of several braided river systems in Alaska obtained via synthetic aperture radar (SAR) imagery confirmed this hypothesis (Nykanen *et al.*, 1998). For example, Figure 5 shows two reaches of the Tanana River in Alaska and the corresponding plots that test for the presence of spatial scaling. In Reach C (left plot), a mountainous region adjacent to the river exerts an external control (contrary to internal self-organizing mechanisms creating the braiding). Reach D (right plot) has a very gradual slope and a low braiding index (3.14 vs. 5.22 for the previous reach). Although no morphological constraints seem present, this is a transitional river reach connecting a fully braided regime to a single meandering river regime. Thus this reach is characterised by a single dominant channel throughout its length. The width of that main channel is approximately ten times that of the next biggest channel, with all intermediate channel widths missing. As seen in Figure 5, spatial scaling is not present here either. Along the same Tanana river, reaches which do not exhibit the above topographic or transitional controls exhibit very good spatial scaling (Nykanen *et al.*, 1998).

2.3 Dynamic (time-space) scaling

The analysis of the preceding section indicates clearly that the planform of braided rivers shows self-affine scaling if the river systems are left to evolve undisturbed and no external controls influence their development. As informative as this is, it is nonetheless restricted to static planforms. A more complete understanding of the physics of braided rivers requires an understanding of how the scaling can be extended to time. It is clear from watching braided rivers that they evolve with time, through small incremental changes that cumulatively produce larger changes by, for instance, diverting water from one part of the network to another. Is there a temporal scaling as well, and if so how is it related to the spatial scaling?

This question was first tackled by Sapozhnikov and Foufoula-Georgiou (1997), who posed the question as follows. Consider two movies, one of a small section of a braided river, with length scale L_1 and the other of a larger section with length scale L_2. Now compare the two movies by, say, projecting them onto adjacent screens (at the same size). Intuitively one would expect the smaller-scale movie to seem to evolve faster than the large-scale one, because it should take longer for the larger channels to move some representative distance,

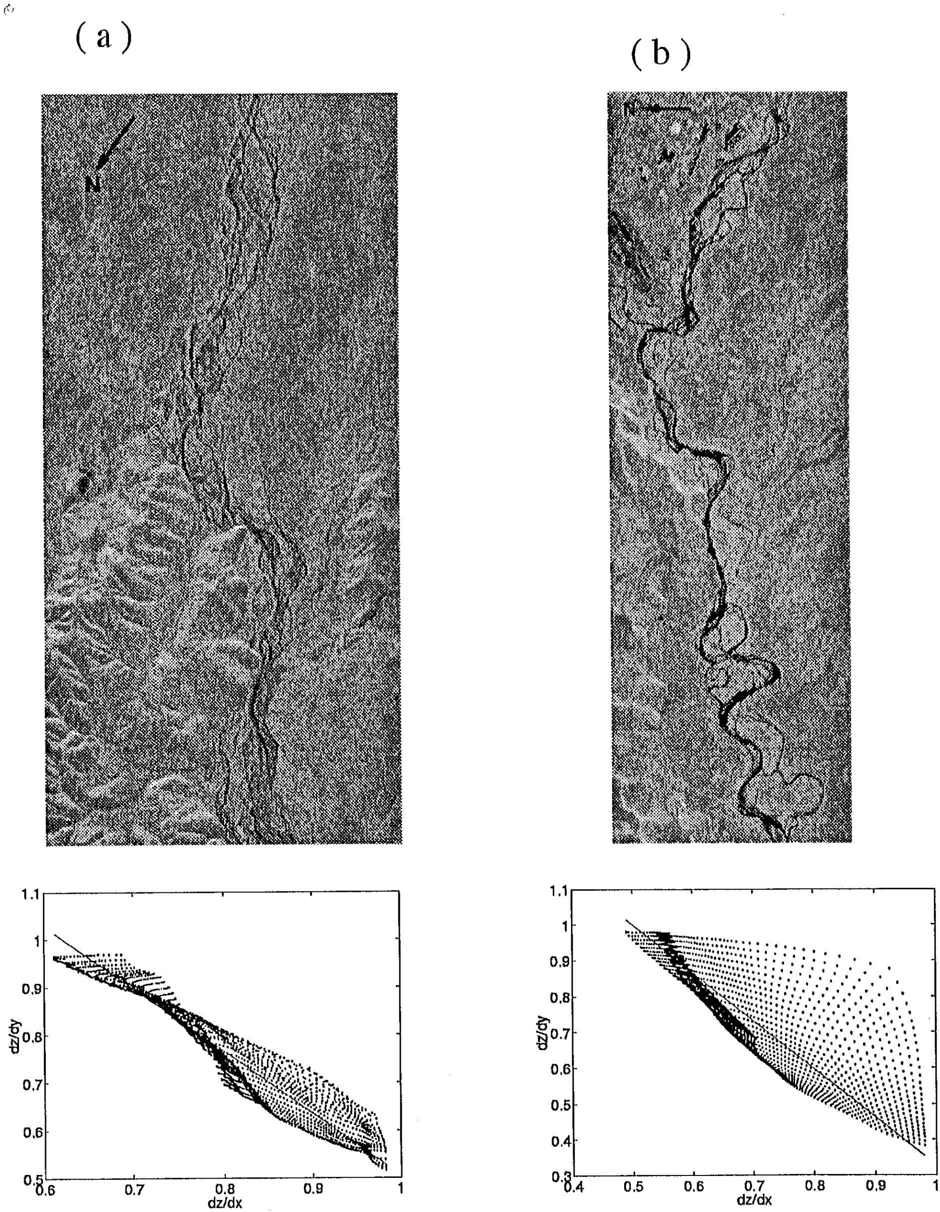

Figure 5. Two reaches of the Tanana River (Alaska), and associated LCI plots, showing breakdown in scaling due to (a) imposition of a geological control, and (b) development of a single dominant channel associated with transition to meandering.

e.g. one channel width. Now suppose you had a speed control for the smaller-scale movie. Could you, by slowing it down, make it statistically indistinguishable from the larger-scale movie? If so, how would the magnitude of this 'slow-motion' factor be related to the spatial scale ratio L_2/L_1? Sapozhnikov and Foufoula-Georgiou (1997) proposed that, if T_1 and T_2 are time scales for the two cases (i.e. T_2/T_1 is the 'slow-motion' factor), the presence of statistical space-time scaling implies a space-time rescaling such that

$$\frac{T_2}{T_1} = \left[\frac{L_2}{L_1}\right]^z \tag{1}$$

where z is a scaling exponent. The presence of such a statistical scale invariance under a power law space-time transformation is called dynamic scaling. The next question is how to test quantitatively for the presence of dynamic scaling in braided river systems.

Sapozhnikov and Foufoula-Georgiou (1997) proposed a methodology based on the probability distributions of temporal changes in the patterns of braided rivers. Changes were defined as parts of the space which were either not occupied by water but became occupied, or were occupied but became dry, or in which depth changes caused a change in dye concentration, after some time lag t. If $n(l' > l, t)$ denotes the number of changes larger than size l (where size is quantified by the square root of the area of the change) then it can be shown (Sapozhnikov and Foufoula-Georgiou, 1997) that the condition of dynamic scaling above can be written in terms of the statistics of changes as:

$$n(l' > l, t) = l^{-D} f\left[\frac{t}{l^z}\right] \tag{2}$$

where $f(.)$ is an unknown function, and D is the fractal dimension of the braided river spatial pattern. A step-by-step method for estimating the dynamic scaling component z is presented in Sapozhnikov and Foufoula-Georgiou (1997). Suffice to say that for given estimates of D and z, the presence of dynamic scaling implies that $n(l' > l, t)\, l^D$ vs. t/l^z for different values of the time lag t and for different sizes of pattern changes should all collapse on the same curve $f(.)$. As will be demonstrated below, this holds true for data from an experimental braided river, implying the presence of dynamic scaling.

The difficulty of obtaining the necessary observations of the evolution of natural braided rivers in the field, and the resolution limitations of satellite images, suggest using laboratory data to begin the search for dynamical scaling. It is relatively easy to produce small-scale laboratory braided river networks that show essentially all of the morphological and dynamic characteristic of their field-scale cousins. From a hydraulic point of view this can be rigorously justified on the basis of the Froude scale modeling (Ashmore, 1982). Details of the experiments discussed here are in Sapozhnikov and Foufoula-Georgiou (1997). The experimental basin was 5 m × 0.75 m and was continuously supplied with sediment (median grain size = 0.12 ± 0.03 mm with a discharge of 0.6 g/s) and water (discharge 20 g/s). A video camera recorded the evolution of the system. To visualise the river and monitor its depth, dye was supplied continuously during each videotaping session. After each videotaping session, the dye supply was cut and water flushed the dye from the system in a matter of a few hours. The recorded data were consequently digitised for treatment and analysis. The study region was 0.75 m wide and 1.0 m long and began 2.8 m downstream of the feed point. The final resolution of the images (Figure 6) was 3 mm across the river and 1.5 mm along the river.

Figure 6. Photograph of the experimental braided river used to measure the time-space distribution of changes (from Foufoula-Georgiou and Sapozhnikov, 2001).

Using the mass-in-a box method (Mandelbrot, 1982; Sapozhnikov and Foufoula-Georgiou, 1997) the fractal dimension of the braided river was estimated to be $D = 1.75$. Using the step-wise-estimation procedure (Foufoula-Georgiou and Sapozhnikov, 2001; Sapozhnikov and Foufoula-Georgiou, 1997) the dynamic scaling exponent was then estimated to be $z \cong 0.5$. Using these values of D and z, the plot of the rescaled distributions is shown in Figure 7. All curves (rescaled probability distributions) collapse to a single curve, providing full evidence for the presence of dynamic scaling.

The physical interpretation of the value of the dynamic scaling exponent was extensively discussed in Sapozhnikov and Foufoula-Georgiou (1997). They compared their estimate of $z \cong 0.5$ with two limiting cases: A value of $z = 2$ would suggest that the time scale of changes is controlled by a diffusion-type process and is thus proportional to the square root of the length scale of the changes. A value of $z = 0$ would indicate that no rescaling would be needed

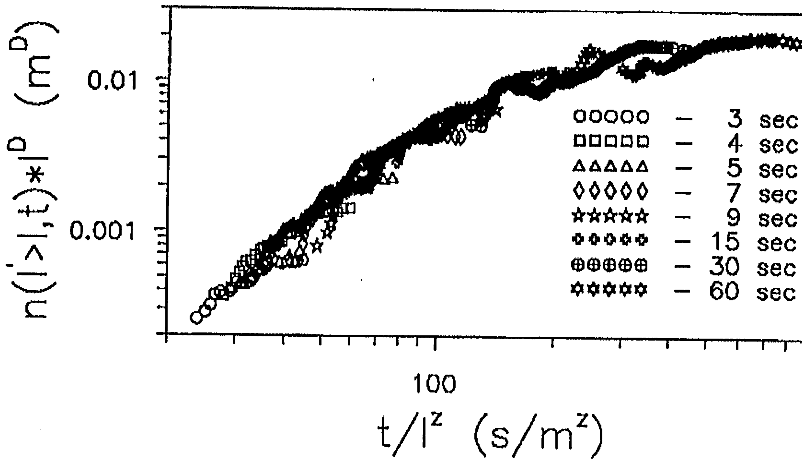

Figure 7. **Number of occurrences of events of a given size for the experimental braided river in Figure 6, rescaled using estimated values of the fractal dimension $D \cong 1.75$ and the dynamic-scaling exponent $z = 0.5$. The distribution functions collapse onto a single line, verifying the presence of dynamic scaling (from Foufoula-Georgiou and Sapozhnikov, 2001).**

going from a small to a larger spatial scale, i.e. the time scale of changes of all sizes is the same. The relatively small value $z \cong 0.5$ implies that, although small changes do have a shorter time scale than large ones, the difference is much less than one would expect if the time scaling behaved diffusionally. Sapozhnikov and Foufoula-Georgiou (1997) suggested that the evolution of small features is largely controlled by the evolution of larger ones. We will return to this point below.

3. IMPLICATIONS OF SCALING

What does it mean that braided rivers show evidence of both static and dynamic scaling? What does it mean if they are self-organised critical (SOC)? We will begin with the latter question, because in a sense it contains the answer to the first question: although scaling does not by itself imply SOC, SOC does imply both the time-space scaling and fractal spatial patterns described in the previous sections.

The direct meaning of SOC is implied in the definition: the system organises itself in such a way that it brings itself to a "critical" state in which small perturbations produce response over all possible length scales in the system. The frequency of these responses depends on an inverse power of the size of the response.

The original SOC model (Bak *et al.*, 1987) was illustrated using an imaginary sand pile. This archetypal system, which turns out to have little to do with real sand piles, has two essential features: (1) it is *two-dimensional*, and (2) it has a *nonlinear* (via a threshold slope) law for particle motion. Both of these features seem to have clear analogues in braided streams. Braided streams are fundamentally two-dimensional: much of their dynamics arises from the interaction of different flow threads, which obviously could not arise without a second dimension to provide for variable paths. It is tempting to point to the well known threshold shear stress for initiating sediment motion as the analogue for Bak *et al.*'s threshold slope, but in our view this would be misleading — it would imply that braiding could occur only for conditions near critical, which is patently not the case for sand-bed, suspension dominated braided rivers like the Brahmaputra. We suggest instead that the essential feature is non-linearity of transport, a property fundamental to all useful sediment transport laws and one identified as fundamental to braiding for other reasons by Murray and Paola (1994). The steep increase of sediment flux with flow velocity u (e.g. as u^5 in the Engelund-Hansen (1967) total load law) plays the same role in stream braiding as the on-off behaviour invoked by Bak *et al.* in their sand-pile model.

So it seems that two very basic properties of braided rivers are consistent with the existence of SOC behaviour. What good does it do us to know that braided rivers may be SOC? One important advantage of identifying a "generic" behaviour like SOC is that, once proven, it implies a number of system attributes, like power-law scaling and fractality, that are useful in modeling and prediction. That characteristics like these are common to all SOC systems also implies that we may be able to apply results from other, better studied SOC systems to the braided river problem.

3.1 SOC and sediment flux

The SOC nature of braided rivers has implications for the way in which they convey material. A number of workers have noted that sediment flux in braided rivers is highly variable in time. These sediment pulses have been observed in both laboratory and field measurements (Ashmore, 1991; Goff and Ashmore, 1994; Hoey, 1992; Hoey and Sutherland, 1991). Similar pulses developed spontaneously in the braided river model of Murray and Paola (1994), suggesting that they are a generic feature of sediment transport in braided rivers. Here we will show that the avalanches of the original Bak *et al.* (1987) two-dimensional sandpile model lead directly to transport pulses in that model as well. In the original model, the system was "probed" by dropping single particles on it at random locations. A simple change to this setup is to supply the system with a steady flux of material at one end and then monitor the flow rate of particles from the other end. The rules are otherwise the same as in the Bak *et al.* model. The result of this is shown in Figure 8a. The output flow rate, on average, equals the feed rate, but is clearly quite variable. This variability is induced by storage and release of material as a result of the slope threshold for avalanching. A similar storage and release mechanism is thought to be responsible for producing the fluctuations in sediment output of braided streams, but evidently (Figure 8b) it produces a significantly lower level of intermittency than in the sandpile model.

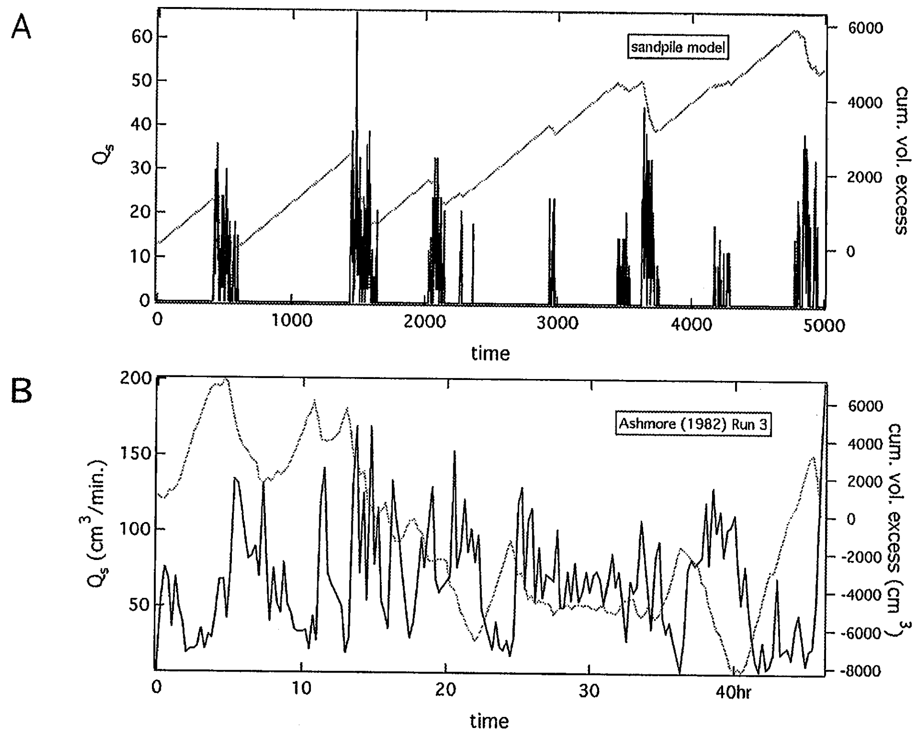

Figure 8. **Sequences of sediment output (black) from (a) the original Bak *et al.* (1987) sandpile model with steady sediment supply and (b) an experimental braided river (Ashmore, 1985). The grey lines in the background show cumulative excess mass (cumulative input – output) in each system.**

In the Bak *et al.* (1987) model, there is only one material type in transport. Braided rivers transport both water and sediment. Although obviously these two phases are closely coupled, they have quite different time scales. The events studied by Sapozhnikov and Foufoula-Georgiou are changes in the plan-view distribution of water. To what extent are water events and sediment events coupled? The observations of Ashmore (1985) establish a general connection between sediment pulses and areas of rapid change in channel pattern. However, this connection has not been explored in detail. Although it is possible in principle to have high sediment flux events without changing the bed topography substantially, the general connection between sediment pulses and the growth and incision of bars suggests that this is unlikely. On the other hand, our observation is that it is possible to change the flow pattern dramatically with only a minor change in bed topography, if a small change occurs in an advantageous location. Further study of the relation among topographic change, sediment flux pulses, and change in flow pattern should be an extremely fruitful area in braided river research.

3.2 SOC and flooding

One important practical application of SOC is to predict the likelihood of changes of various magnitudes. Anyone charged with designing structures in or around braided rivers must be able to estimate the recurrence interval or probability of flows of various magnitudes at a given point in the system. This problem has a very different structure in a braided river than in one with a fixed or slowly evolving channel. In the latter, which is the conventional case considered by river engineers, flooding statistics are controlled by the likelihood of discharge events of a given magnitude, along with the geometries of the channel and floodplain. In an active braided stream, the likelihood of flooding at a given point depends both on discharge statistics and on the statistics of channel shifting. The channel shifting statistics are controlled by the internal dynamics of the river system and would lead to flooding everywhere even if the discharge never changed (Cazanacli, 2000). Understanding the SOC nature of braided rivers is essential to constraining this piece of the flooding problem.

We can gain some further insight into applying SOC concepts to evaluating flood risk by turning to one of the best-studied SOC systems: geological faults. Fault systems were one of the first physical systems proposed to show SOC behaviour (Olami *et al.*, 1992; Sornette, 1992). Here the "avalanches" correspond to earthquakes, and the power law distribution of avalanche sizes to the well known Gutenberg-Richter law of earthquake magnitude. One result of earthquake research is that, despite enormous effort driven by a compelling social need, it is still not possible to predict specific earthquakes, and there is at present little prospect of doing so. So at this point, it does not seem that there is much chance of predicting specific changes in braided river patterns either. On the other hand, it is quite possible to quantify seismic hazard, and likewise, it should be possible to quantify risk associated with stream braiding as well.

Adopting this approach, the first question is how to quantify the general risk of flooding for areas within the braid plain. As mentioned above, in braided rivers the probability of flooding in a particular area depends both on variation in discharge and on the probability of occurrence of a flow path at the point in question. The latter is associated with the internal dynamics of the system. Channel shifting on relatively short time scales implies that braided rivers would eventually wet their entire braid plain even if their discharge never changed. Our group at St. Anthony Falls Laboratory (Cazanacli, 2000) has analysed the probability of successive occupation of unwetted areas for an experimental braided fan. The most important result of this work is that unwetted area on the fan surface decays according to:

$$f_{dry}(t) = \frac{f_{dry}(0)}{1 + t/T_{cm}} \qquad (3a)$$

where $f_{dry}(t)$ is the fraction of the total fan area that has never been under water in the time interval $[0, t]$, and T_{cm} is a channel-mobility time scale given by:

$$T_{cm} = \frac{\alpha B_a h(B_T - B_a)}{Q_s} \qquad (3b)$$

where α is an order-one coefficient (empirically $\alpha \cong 1.8$), B_a is the total width of active channels, h, is the mean channel depth, B_T is the total width of the braid plain or fan, and Q_s is the total sediment flux. The physical reasoning behind a similar time scale is discussed in Paola (2001).

Equations (3a, b) have been tested only for two rates of deposition in a single experiment. If the basic form and physical basis prove general, then they can be used to quantify that part of the flooding hazard within a braided system associated with flow switching, on the basis of readily measurable physical quantities.

The harder problem of calculating the likelihood of a shift in the river pattern of a given size can be tackled using the results of dynamic-scaling analysis. The rescaling presented in Figure 7 implies that the probability of high-magnitude, low-frequency events can be estimated from relatively straightforward measurements of the distribution of smaller, more frequent events (Sapozhnikov and Foufoula-Georgiou, 1997). We begin by establishing the function $n(l_1, t_1)$ that gives the number of changes exceeding a characteristic length scale l_1 (measured, for instance as the square root of the area of the change) between photographs or maps of a river taken some relatively short interval t_1 (e.g. one year) apart. (The discharge must be the same in the two images to make the comparison useful.) It is unlikely that we will observe any extremely large shifts in this short time, but we can establish the form of $n(l_1, t_1)$. Now we want to use this to estimate the likelihood of (generally larger) changes l_2 occurring over some longer time interval t_2 (e.g. 10 years). According to equation (1), the length must be rescaled as $l_2 = l_1(t_1/t_2)^{1/z}$. With $z \cong 0.5$, this means, for instance, that a length scale of 1 m over a year is equivalent to a length scale 100 m over 10 years. This gives the distribution $n(l_2, t_2)$ The length of the box over which the changes are counted must be scaled up the same way, so 100 m by 100 m becomes 10 km by 10 km. Because the planform is a fractal with dimension D, the number of changes in the longer-term, larger-scale case must be scaled with $(l_2/l_1)^D$. (The rescaling really should account for self-affinity (Foufoula-Georgiou and Sapozhnikov, 1998) but this complicates matters considerably.) Thus, if in our one-year comparison with a 100 m box there were 5000 changes with length scale > 1m, this would imply that on a ten-year comparison with a 10 km box the number of changes with a length scale > 100 m would be $1.58 = 5000/(100^{1.75})$.

We return to the earthquake analogy for a more speculative avenue for assessing the risk of a large event. For earthquakes, a basic measure of risk is based on adding up the accumulated strain since the last large event. This provides an estimate of the largest event the system is capable of producing. In a braided river or a sandpile model, the analogue of accumulated strain is accumulated sediment mass. So one could ask how the likelihood of a sediment transport event of a given size depends on the accumulated mass excess since the last avalanche of that size. The incremental mass excess at each time t is $dQ_s(t)\Delta t = (Q_{s0} - Q_s(L,t))\Delta t$ where $Q_s(x,t)$ is the mass discharge summed over each row of cells, Q_{s0} is the (constant) supply value, and L is the length of the system. The accumulated mass excess for the i^{th} event of magnitude $\geq M$ is

$$\mathrm{D}t \sum_{t=ti,M}^{ti+1,M} dQ_s(t_{i,M}) \tag{4}$$

where $t_{i,M}$ is the time of the event, and $t_{i+1,M}$ is the time of the next event $\geq M$.

Figure 8 shows time series of accumulated volume (mass) excess for the steadily forced sandpile model and an experimental braided river (Ashmore, 1985). The sandpile results are based on a sequence of 11,000 values of the output sediment flux $Q(L,t)$. Average event size is compared with cumulative mass excess for both cases in Figure 9a. For the sandpile, there is a relation between event magnitude and accumulated mass excess, but the mass excess is typically much larger than any individual event. This is in contrast to the earthquake case, where large earthquakes seem to "flush" the system of accumulated strain. In the forced sandpile model the flushing occurs instead via a whole cluster of transport events. Figure 9b shows the results of a similar analysis of the bedload flux time series shown in Figure 8b, as well as one additional experimental run. For these relatively short sequences, the results are sensitive to where the mass accounting is started and stopped. We began the

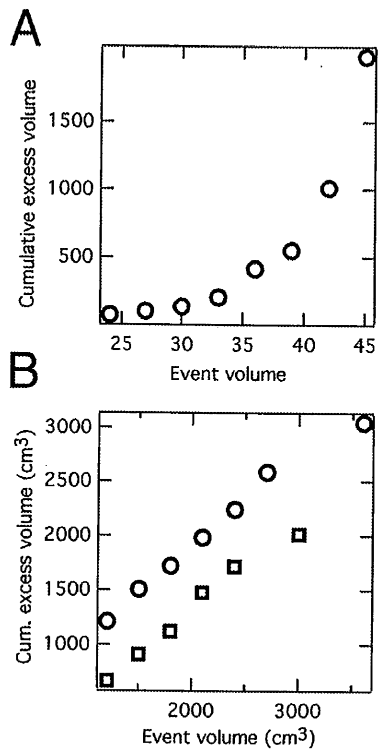

Figure 9. **Sediment volume for specific discharge events compared with accumulated excess volume (Figure 8) for (a) forced sandpile model and (b) two runs from an experimental braided river (Ashmore, 1985; circles, run 11; squares, run 3). In the latter case the discharges were averaged over 15 minutes.**

mass balance with a low value that followed a series of large events, in order to study how the system built up to the next major event. Figure 9b shows that for this case the sizes of the output events were comparable to the accumulated mass excess. Evidently the monitoring interval (15 minutes) in the experiments was long enough to encompass major mass-clearing episodes of sediment flux. While these results are only preliminary, they suggest that the likelihood of major flux events might be estimated from careful monitoring of the sediment budget of a braided river. The flux events are of interest in their own right, but insofar as they are associated with major reorganisations in the flow pattern they could be important in evaluating flood hazard as well.

3.3 SOC and scale dependence of channel activity

Sapozhnikov and Foufoula-Georgiou (1997) pointed out that their finding that the temporal exponent z was about 0.5 implies that the dependence of characteristic time on length scale is relatively weak. They speculated that this might imply that changes at smaller scales are strongly forced by changes at larger scales. Another way of looking at this is to ask what $z = 0.5$ implies if the observed changes are limited by rates of sediment transfer. One would expect the unit volumetric flux q_s to scale as $q_s \sim L^2/T$ so characteristic fluxes on length scales L_1 and L_2 should scale as

$$\frac{q_{s_2}}{q_{s_1}} = \left(\frac{L_2}{L_1}\right)^2 \left(\frac{T_2}{T_1}\right)^{-1} \tag{5}$$

which implies, with $z = 0.5$ (equation 1),

$$\frac{q_{s_2}}{q_{s_1}} = \left(\frac{L_2}{L_1}\right)^{3/2} \tag{6}$$

If sediment flux scales with boundary shear stress τ as $q_s \sim \tau^{3/2}$, then the characteristic stress decreases with length scale as $\tau \sim L$. So small events are associated with small local stresses. If local flow depth scales as L, and stress is controlled by the depth-slope product, the implication of $\tau \sim L$ is that there is no correlation between local slope and event size. This inference should be easy to check.

3.4 The limits to scaling

Static scaling of braided rivers has been demonstrated over a range of less than two orders of magnitude in length scale (Sapozhnikov and Foufoula-Georgiou, 1996). The upper limit to scaling is set by the width of the braid plain, which in turn is set in most cases by tectonic or other outside controls. The maximum length scale of braiding itself—the "integral scale"—seems to correspond to the fundamental bar wavelength as identified in classical analyses of linear instability (Ashmore, 2001; Fredsoe, 1978; Parker, 1976). What sets the lower limit, the "Kolmogorov scale" of braiding? For analyses like that of Sapozhnikov and Foufoula-Georgiou (1996), the effective lower limit is the resolution of available air photos; the real physical limit is not known. At this point we can only offer some suggestions as to the likely controls on the fine scale of braiding. Some of the fine structure comprises small remnant flows in channels that have been largely abandoned. These are passive features, although they may be important as havens for deposition of fine sediments. Actively maintained fine structure would have to be able to generate shear stresses above the critical value for sediment transport. One possibility is that small channels are associated with higher slopes, in which case the Kolmogorov scale would be controlled by variance in slope. Otherwise, the range of active channel scales would depend on the range of grain sizes and shear stresses. For gravel bed rivers where the mean shear stress is likely to be near critical for the median size (Parker, 1978), the only means available for extending the range of channel sizes would appear to be formation of local patches of fine sediment that could remain mobile with smaller stresses (Paola and Seal, 1995). For sand-bed rivers the mean dimensionless stress is more typically in the range of 20-50 times critical (Parker *et al.*, 1998). In this case it should be possible to maintain a range of active channel sizes over more than a decade in length scale even with no variation in grain size or characteristic slope.

4. FURTHER WORK AND NEW DIRECTIONS

The research described here represents an initial analysis of the statistical geometry of braided rivers. Some avenues that we think would be particularly rewarding for future research include:

1. Can we develop a predictive, mechanistic theory that relates both static and dynamic scaling behaviour to imposed conditions such as sediment and water flux or grain size?
2. How can we extend scaling ideas to the vertical dimension, using for example newly available high-resolution topographic data (e.g. Lane, 2001)? This could allow us, for instance, to predict the likelihood of large depth changes from measurements of smaller ones.
3. Can we develop a predictive theory for the breakdown of scaling by imposed controls, including bedrock, tectonic controls and vegetation?
4. Can we use presence/absence of scaling in natural river systems to identify disturbed areas? Could approach to scaling be useful as a measure of the recovery of a river section after disturbance?
5. Is there scaling in other variables such as velocity field and local grain size, beyond that imposed by the forms of scaling that have already been identified?

6. What are the implications of static and dynamic scaling for the stratigraphic record of braided rivers?

5. ACKNOWLEDGEMENTS

We are grateful to Brad Murray and Victor Sapozhnikov for their help with this paper. The research was supported by NSF grant EAR 96-28393 and NASA grant NAG-6191. Computational resources were provided by the Minnesota Supercomputer Institute (MSI).

6. REFERENCES

Alciatore, D., and Miranda, R., 1995. The best least-squares line fit. In Paeth, A. W. (editor), *Graphics Gems V*, pp. 91-97. Academic, San Diego.

Ashmore, P., 1991. Channel morphology and bed load pulses in braided, gravel-bed streams. *Geografiska Annaler* 73A, 37-52.

Ashmore, P. E., 1982. Laboratory modelling of gravel braided stream morphology. *Earth Surface Processes and Landforms* 7, 201-225.

Ashmore, P. E., 1985. Process and form in gravel braided streams: laboratory modelling and field observations. Ph. D. thesis, University of Alberta.

Ashmore, P.E., 2001. Braiding phenomena: statics and kinetics. In: Mosley, M. P., (editor), *Gravel Bed Rivers V*. New Zealand Hydrological Society, Wellington.

Bak, P., Tang, C., and Wiesenfeld, K., 1987. Self-organized criticality: an explanation for 1/*f* noise. *Physics Review Letters* 59, 381-384.

Cazanacli, D. A., 2000. Experiment on flow in a steep, braided stream: application to flooding risk on alluvial fans. M. S. thesis, University of Minnesota.

Engelund, F., and Hansen, E., 1967. *A Monograph on Sediment Transport in Alluvial Streams*. Teknisk Forlag, Copenhagen, 62 pp.

Foufoula-Georgiou, E., Sapozhnikov, V. B., 1998. Anisotropic scaling in braided rivers: an integrated theoretical framework and results from application to an experimental river. *Water Resources Research* 34, 863-867.

Foufoula-Georgiou, E., and Sapozhnikov, V. B., in press. Scale invariances in the morphology and evolution of braided rivers. *Mathematical Geology*.

Fredsoe, J., 1978. Meandering and braiding of rivers. *Journal of Fluid Mechanics* 84, 609-624.

Goff, J. R. and Ashmore, P., 1994. Gravel transport and morphological change in braided Sunwapta River, Alberta, Canada. *Earth Surface Processes and Landforms* 19, 195-212.

Hoey, T., 1992. Temporal variations in bedload transport rates and sediment storage in gravel-bed rivers. *Progress in Physical Geograpy* 16, 319-338.

Hoey, T. B., and Sutherland, A. J., 1991. Channel morphology and bedload pulses in braided rivers: a laboratory study. *Earth Surface Processes and Landforms* 16, 447-462.

Howard, A. D., Keetch, M. E., and Linwood, V., 1970. Topological and geometrical properties of braided streams. *Water Resources Research* 6, 1647-1688.

Lane, S. N., 2001. The measurement of gravel bed river morphology. In: Mosley, M. P., (editor), *Gravel Bed Rivers V.* New Zealand Hydrological Society, Wellington.

Mandelbrot, B. B., 1982. *The Fractal Geometry of Nature.* W. H. Freeman and Company, San Francisco, 460 pp.

Murray, A. B., and Moeckel, R., 1997. Measuring the distance between time series. *Physica D*, 102, 187-194.

Murray, A. B., and Paola, C., 1994. A cellular model of braided rivers. *Nature* 371, 54-57.

Murray, A. B., and Paola, C., 1996. A new quantitative test of geomorphic models, applied to a model of braided streams. *Water Resources Research* 32, 2579-2587.

Nykanen, D., Foufoula-Georgiou, E., and Sapozhnikov, V. B., 1998. Study of spatial scaling in braided river patterns using synthetic aperture radar imagery. *Water Resources Research* 34, 1795-1807.

Olami, Z., Feder, H. J. S., and Christensen, K., 1992. Self-organized criticality in a continuous, nonconservative cellular automaton modeling earthquakes. *Physics Review Letters* 68, 1244-1247.

Paola, C., 2001. Modelling stream braiding over a range of scales. In: Mosley, M. P., (editor), *Gravel Bed Rivers V.* New Zealand Hydrological Society, Wellington.

Paola, C., and Seal, R., 1995. Grain-size patchiness as a cause of selective deposition and downstream fining. *Water Resources Research* 31, 1395-1407.

Parker, G., 1976. On the cause and characteristic scales of meandering and braiding in rivers. *Journal of Fluid Mechanics* 76, 457-480.

Parker, G., 1978. Self-formed straight rivers with equilibrium banks and mobile bed. Part 2. The gravel river. *Journal of Fluid Mechanics* 89, 127-146.

Parker, G., Paola, C., Whipple, K. X., and Mohrig, D. C., 1998. Alluvial fans formed by channelized fluvial and sheet flow. I: theory. *Journal of Hydraulic Engineering* 124, 985-995.

Seminara, G., Tubino, .M, and Paola, C., 2001. The morphodynamics of braiding rivers: experimental and theoretical results on unit processes In: Mosley, M. P., (editor), *Gravel Bed Rivers V.* New Zealand Hydrological Society, Wellington.

Sapozhnikov, V. B., and Foufoula-Georgiou, E., 1995. Study of self-similar and self-affine objects using logarithmic correlation integral. *Journal of Physics A: Mathematical and General* 28, 559-571.

Sapozhnikov, V. B., and Foufoula-Georgiou, E., 1996. Self-affinity in braided rivers. *Water Resources Research* 32, 1429-1439.

Sapozhnikov, V. B., and Foufoula-Georgiou, E., 1997. Experimental evidence of dynamic scaling and indications of self-organized criticality in braided rivers. *Water Resources Research* 33, 1983-1991.

Sapozhnikov, V. B., and Foufoula-Georgiou, E., 1999. Horizontal and vertical self-organization of braided rivers towards a critical state. *Water Resources Research* 35, 843-851.

Sornette, D., 1992. Self-organized criticality, earthquakes, and plate tectonics. *Physics Review Letters* 69, 1287.

Weigend, A. S., and Gershenfeld, N. A., 1994. *Time-Series Prediction: Forecasting the Future and Understanding the Past.* Addison-Wesley Publishing Co., Reading, Mass., 630 pp.

APPENDIX: SELF-AFFINITY TESTING

Let X and Y be the sides of a rectangle and $M(X,Y)$ be the mass (e.g., the number of pixels covered by water) of the part of the object contained within the $X \times Y$ rectangle. Then, spatial scaling implies that

$$M(X,Y) \sim X^{1/\nu_x} \sim Y^{1/\nu_y} \qquad \text{(A1)}$$

where ν_x and ν_y are the fractal exponents corresponding to the X and Y directions, respectively. Note that according to Eq. (A1), the mass $M(X,Y)$ scales with the sides of the rectangle only if X scales with Y in a certain way. Equation (A1) can be written in the form

$$\left[\frac{X_2}{X_1}\right]^{1/\nu_x} = \left[\frac{Y_2}{Y_1}\right]^{1/\nu_y} = \frac{M_2}{M_1} \qquad \text{(A2)}$$

If we introduce $x = \log, X$, $y = \log Y$, and $z = \log M$, we get

$$\frac{x_2 - x_1}{\nu_x} = \frac{y_2 - y_1}{\nu_y} = z_2 - z_1 \qquad \text{(A3)}$$

or

$$\frac{dx}{\nu_x} = \frac{dy}{\nu_y} = dz \qquad \text{(A4)}$$

The function $M(X,Y)$ is known as the correlation integral, and by analogy we call the function $z(x,y)$ the logarithmic correlation integral of the object under study. Comparing Equation (A4) with

$$\frac{dz}{dx}dx + \frac{dz}{dy}dy = dz \qquad \text{(A5)}$$

we obtain

$$\nu_x \frac{dz}{dx} + \nu_y \frac{dz}{dy} = 1 \qquad \text{(A6)}$$

This relationship provides a method for testing the presence of spatial scaling and for estimating the fractal exponents ν_x and ν_y of a self-affine object, as follows. Having estimated the logarithmic correlation integral $z(x,y)$ from a pattern of the object by direct calculation of the mass $M(X,Y)$ (i.e., pixels covered by water) within rectangles of sizes $X \times Y$, one can calculate the derivatives $\partial z(x,y)/\partial x$ and $\partial z(x,y)/\partial y$ and use them to test whether the linear relationship (Equation A6) is satisfied and, if yes, to find the values of v_x and v_y. As can be seen from the above equation, $1/v_y$ is the intercept of the linear best fit line with the vertical axis, and $-v_x/v_y$ is the slope. Ideally, only two points are needed to estimate v_x and v_y , but for a good estimation a least squares fit to the derivatives at all points of the surface $z(x,y)$ is preferable. Since both coordinates contain uncertainty in their values, we use a least-squares method which minimises the sum of the squares of the perpendicular to the best-fit line distances (Alciatore and Miranda, 1995).